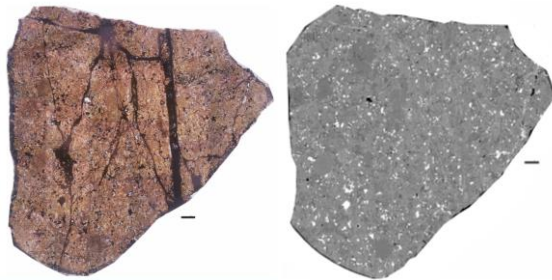


**COMPOSITIONAL AND RAMAN STUDY OF HIGH-PRESSURE MINERALS IN SHOCKED L6 CHONDRITE NORTHWEST AFRICA 12841.** I. Baziotis<sup>1</sup>, L. Ferrière<sup>2</sup>, C. Ma<sup>3</sup>, J. Hu<sup>3</sup>, D. Palles<sup>4</sup>, E. Kamitsos<sup>4</sup>, and P. D. Asimow<sup>3</sup>, <sup>1</sup>Dept. of Natural Resources Management & Agricultural Engineering, Agricultural Univ. of Athens, Iera Odos 75, 11855 Athens, Greece (ibaziotis@aua.gr), <sup>2</sup>Natural History Museum Vienna, Burgring 7, 1010 Vienna, Austria, <sup>3</sup>California Inst. of Technology, Division of Geological & Planetary Sciences, Pasadena, California 91125, USA, <sup>4</sup>Theoretical & Physical Chemistry Inst., National Hellenic Research Foundation, 11635 Athens, Greece.

**Introduction:** The most commonly recovered type of meteorite, ordinary chondrites, often contain a large number of high-pressure (HP) phases as the result of impact events due to collision(s) among their parent asteroids. The L6 subgroup have yielded the most extensive evidence of such shocks. The discovery and characterization of HP minerals, often found in melt veins (MVs), in these meteorites help to constrain the shock conditions and hence parameters of impactors and targets. Herein, we report the discovery of numerous HP minerals in the L6 ordinary chondrite Northwest Africa (NWA) 12841 (find 2010; S4). Many MVs occur in the studied polished thin section (NHMW-O1154), with the widest one having a nearly constant thickness of ~500  $\mu\text{m}$  on the section, while the thinner MVs are variable in width, from a few  $\mu\text{m}$  up to ~200  $\mu\text{m}$  (Fig. 1).



**Figure 1:** Optical microscope (plane-polarized light; left image) and back-scattered electron (BSE; right image) mosaics of the NWA 12841 section showing the thick MV and various thinner MVs. Scale bar in both images is 1 mm.

There is no evidence of cross-cutting relations to suggest that these veins are of multiple generations. The numerous HP minerals identified are used to constrain the complex impact history of NWA 12841.

**Petrography, mineral chemistry, and Raman spectroscopy:** We analyzed 17 regions of interest in the widest MV and in two thinner MVs. A number of techniques – optical microscopy, scanning electron microscopy with co-located electron microprobe (EPMA), Raman spectroscopy (RS) (514 nm laser), and (where possible) electron back-scatter diffraction – were used to characterize the texture of the MVs and the chemistry and structure of the minerals they contain.

The groundmass of NWA 12841 is brownish in color with numerous chondrules. The chondrules are mostly fractured and include barred olivine and

porphyritic olivine-pyroxene types. The groundmass olivine grains show mosaicism and planar deformation features. The thick (main) MV and minor MVs with other orientations are presumed to be the result of a unique shock event; they are mostly in contact with olivine and pyroxene and occasionally with metal. The MVs consist of glass, silicate clasts, sulfides, chromite, phosphate, and Fe-Ni metal. In plane-polarized light, large blue ringwoodite clasts (up to ~100  $\mu\text{m}$ ) are clearly visible within the MVs (Figs. 2A&B). Two melt pockets are also visible within the studied section (Fig. 1).

**HP minerals.** We identified and characterized various HP minerals including ringwoodite (*rwd*), wadsleyite (*wds*), majorite-pyroxene (*maj*), akimotoite (*aki*?)<sup>1</sup>, albitic jadeite (*ab-jd*), lingunite (*lgn*), xieite (*xi*), and tuite (*tu*) (Figs. 2,3).

**Ringwoodite & Wadsleyite:** The ringwoodite crystals within the melt veins (average  $\text{Fo}_{70}$ ) are generally iron-rich compared to wadsleyite (average  $\text{Fo}_{75}$ ). Matrix olivine in contact with the MV contains ringwoodite lamellae,  $\text{Fo}_{72-75}$ . **Majorite-pyroxene:** The EPMA composition of garnet grains in the large MV show an average majoritic garnet composition  $\text{Ca}_{0.05}\text{Mg}_{3.14}\text{Fe}_{0.87}\text{Al}_{0.02}\text{Si}_{3.92}\text{O}_{12}$ . **Akimotoite (?):** One analyzed grain displays a Raman spectrum consistent with akimotoite (Fig. 4) but a Ca-rich pyroxene composition by EPMA,  $\text{Ca}_{0.83}\text{Fe}_{0.16}\text{Mg}_{0.98}\text{Al}_{0.02}\text{Si}_{1.98}\text{O}_6$ . At this time we have not resolved whether this is a novel high-Ca HP phase or a fine mixture of akimotoite and clinopyroxene. **Albitic jadeite:** The dark grains in the large clast (Fig. 3) in the large MV yield the following empirical formula (based on EPMA analysis):  $(\text{Na}_{0.61-0.66}\text{Ca}_{0.07-0.08}\text{K}_{0.03-0.05}\text{Vac}_{0.22-0.27})(\text{Al}_{0.81-0.83}\text{Si}_{0.16-0.17}\text{Fe}_{0.02-0.03})\text{Si}_2\text{O}_6$ . The M2 vacancies and Si on M1 make this an example of albitic jadeite. **Tuite:** Minute single crystals (2–3  $\mu\text{m}$  in size; Fig. 3H) are associated with apatite and merrillite within a rounded phosphate grain (~100  $\mu\text{m}$  in diameter). The EPMA composition of tuite shows MgO up to ~1.1 wt% and relatively high Cl content, likely due to contamination from adjacent apatite.

The RS of NWA 12841 confirms the presence of *rwd*, *wds*, *maj*, *aki*?, a sodic HP clinopyroxene (RS looks like *jd* but composition is albitic jadeite), *lgn*, *xi*, and *tu*. Each phase matches the characteristic RS bands of reference minerals from the RRUFF database (Fig. 4).

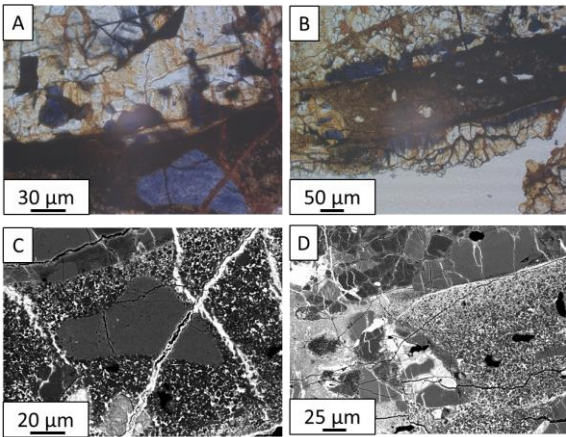


**Figure 2:** Optical microscope images of *rwd* (A) within MV and (B) in contact with the groundmass. BSE images of (C) the polycrystalline blue *rwd* given in (A) and (D) of the numerous *rwd* lamellae within Ol given in (B).

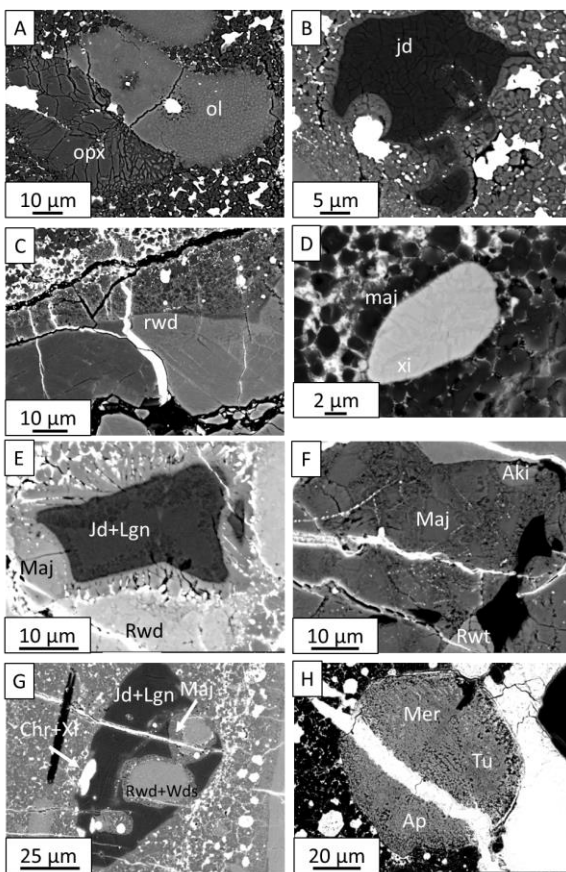


**Figure 3:** BSE images: (A) Large clasts of shocked olivine (*ol*) and orthopyroxene (*opx*). (B) Large albitic *jd* at the edge of MV. (C) Groundmass olivine with *rwd* lamellae in contact with MV. (D) *Xi* crystal (bright areas) within chromite (dark areas) clast surrounded by equigranular majorite. (E) Irregularly shaped clast of albitic *jd+lgn*, surrounded by *maj* and *rwd*. (F) *Maj* and *aki?* in contact with *rwd* within MV. (G) Large clast, composed by numerous HP minerals, within MV. (H) Rounded phosphate clast composed by apatite (*ap*), merrillite (*mer*), and *tu* (verified by RS).

**Implications:** Peak pressure ( $P$ ) and temperature ( $T$ ) conditions of 18-23 GPa and 1800-2100 °C are suggested by the assemblage *maj+rwd*, while *wds* suggests lower  $P$  in the range of 13-18 GPa. The majoritic garnet composition can also be used to estimate pressure based on Collerson's calibration [1]. The EPMA analysis of NWA 12841 *maj*, converted to cation mole fractions on the crystallographic sites, give  $P = 23.0 \pm 0.23$  GPa. The  $P$  estimate using the Collerson's calibration is in good agreement with the peak shock  $P$  inferred from static experiments on the liquidus field of *maj* in chondritic melt compositions. Coexistence of the HP phases indicates small-scale spatial or temporal heterogeneity of the  $P$  field or  $P$ - $T$ - $t$  paths from very high  $T$  during shock to low  $T$  after  $P$  release [2].

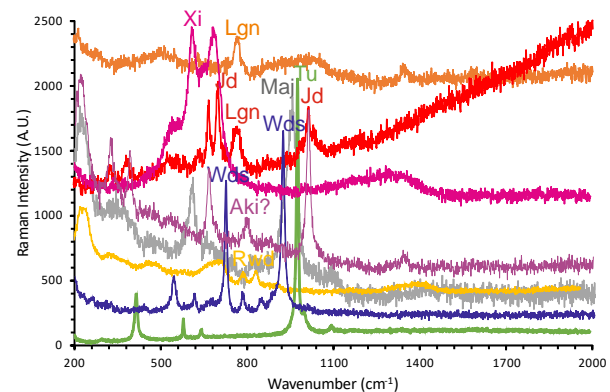


**Figure 4:** Selected RS obtained for NWA 12841 HP minerals.

NWA 12841 hosts a unique record of eight high- $P$ ,  $T$  minerals. The HP minerals and the sizes of their host MVs yield constraints on the  $P$ - $T$ - $t$  path induced in NWA 12841 by the strong shock that passed through it. The assigned peak is in the range  $P = 18$ -23 GPa and  $T = 1800$ -2100 °C. These results contribute to the shock record of the L-chondrites. Additional petrographic work will be conducted to find whether multiple generations of MVs are present in NWA 12841 via cross-cutting relations, in order to test if more than one impact event is recorded in this meteorite.

**Acknowledgments:** I.B. received support from the SYNTHESYS Project which is financed by the European Community Research Infrastructure Action under the FP7 "Capacities" Program. I.B. acknowledges the private company TEMAK S.A. for funding his participation in LPSC 2023. Dan Topa is acknowledged for assistance in the acquisition of EPMA data at the NHMW.

**References:** [1] Collerson K. D. et al. (2010) *GCA*, 74, 5939–5957. [2] Hu J. & Sharp T. (2022) *Prog. Earth Planet. Sci.*, 9:6.